Wave-packet initial motion, spreading, and energy in the periodically kicked pendulum

Boon Leong Lan
Department of Chemistry, Emory University, Atlanta, Georgia 30322
(Received 1 October 1993; revised manuscript received 21 March 1994)

The initial quantum dynamics of an initially well-localized, minimum-uncertainty Gaussian wave packet is studied analytically for the periodically kicked pendulum. The general results presented here include our earlier analytic result [Phys. Rev. A **41**, 2952 (1990)] as a special case. We find that as long as the packet remains localized, it remains approximately Gaussian, while its center and widths evolve in time approximately according to, respectively, the classical map and a variance map which utilize the instantaneous values of the classical Jacobi matrix. When the classical map is very strongly chaotic, we predict that the average kinetic energy of the well-localized wave packet does not initially grow diffusively (linearly with time). We show that, instead, in the presence of chaos, the deviations initially grow, on the average, exponentially at a rate equal to the corresponding classical Liapunov exponent under the appropriate conditions. The time scale (Ehrenfest time) on which the Ehrenfest-Hamilton correspondence holds in the presence of chaos is estimated and is slightly different from a previous estimate made by Chirikov, Israilev, and Shepelyansky [Sov. Sci. Rev. C **2**, 209 (1981)]. Numerical evidence in support of these analytical results is presented.

PACS number(s): 05.45.+b, 03.65.−w

I. INTRODUCTION

Introduced by Chirikov [1], the classical version of the periodically kicked pendulum is a prototype for Hamiltonian chaos. Beginning with Casati *et al.* [2], the quantum version has been intensely studied (see [3–7] for reviews and references) to understand the quantum manifestations of classical chaos. The purpose of this paper is to provide a general analytical framework from which the effect of classical chaos on the initial motion, spreading, and energy of an initially well-localized (in position and momentum), minimum-uncertainty Gaussian wave packet for the kicked pendulum can be understood. Our previous analytic study [8] was limited to the parameter regime for which the classical map is weakly chaotic. The present result is valid for all parameter values of the classical map and it includes our previous result [8] as a special case.

Moreover, the wave-packet propagation method employed here is different from our approach in [8]. Here, we analytically evolve an initially minimum-uncertainty Gaussian wave packet in time by expanding the potential about its instantaneous center and keeping only terms up to the quadratic term. We find that the wave packet remains Gaussian while its center (mean position and momentum) evolves in time according to the classical map, and its widths (variances) evolve in time according to a simple two-dimensional map which utilizes the instantaneous values of the classical Jacobi stability matrix at each iteration [9]. The initial motion and spreading of the *exact* wave packet, i.e., one which evolves in time according to the full Hamiltonian, should be well described by the classical and variance maps, respectively, while its shape remains approximately Gaussian, provided that the instantaneous quadratic approximation to the potential is good which in turn implies that the wave packet should be well localized in angle initially and remain so. These expectations are verified by comparing our previous exact wave-packet numerical results [10] to our present analytical results. We find that the quadratic approximation becomes invalid once the angular deviation (square root of the variance) reaches a saturation value of order 1 rad. Using the variance map, we will show that the wave packet will not remain localized in angle (angular deviation much less than order unity) if it is not also localized in angular momentum.

Numerical quantum dynamical studies by other authors [2,11,12] have shown that, when the classical map is very strongly chaotic, the average kinetic energy grows diffusively at approximately the corresponding classical rate but saturates after some time. This behavior is [2,11,12] typical for a variety of initial states, the ground state of the free rotor being representative. On the other hand, it was also realized [6,11] that special initial states must exist for which diffusion is absent from the outset. An example was given in [6] where the wave packet after diffusion has been suppressed is taken as the initial state. Here, we predict that the kinetic energy of our well-localized wave packet will not grow diffusively initially, but it could, for instance, grow exponentially initially.

In our previous numerical study [10], we found that the initial growths of the deviations are, on the average, exponential with very nearly identical rates in the presence of chaos; in contrast, the initial growths are slower (e.g., linearly) without chaos. Using the variance map, we will show that the rate of exponential growth is equal to the classical Liapunov exponent under the appropriate conditions. We then make an estimate of the time scale (Ehrenfest time) on which the Ehrenfest-Hamilton correspondence (i.e., correspondence between the quantum mean values and the solutions to the classical map) holds in the presence of chaos and find it to be slightly

different from a previous estimate obtained by Chirikov, Israilev, and Shepelyansky [11].

II. CLASSICAL MOTION, SMALL-ERROR PROPAGATION, AND LIAPUNOV EXPONENT

The Hamiltonian for the periodically kicked pendulum is [2,8,10]

$$H=\frac{P^2}{2mL^2}-\delta_p(t/T)mL^2\omega_0^2\cos\theta\ , \tag{1}$$

where

$$\delta_p(t/T)=\sum_{j=-\infty}^{\infty}\delta(j-t/T)$$

is a periodic δ function, T is the kicking period, ω_0 is the small amplitude frequency, and L and m are, respectively, the length and mass of the pendulum. Classically, Hamilton's equation of motion is easily integrated to produce a mapping of the angular momentum P and angle θ from just before the nth kick to just before the $(n+1)$th kick [2,8,10]:

$$P_{n+1}=P_n-\alpha\sin\theta_n\ , \tag{2a}$$

$$\theta_{n+1}=(\theta_n+\beta P_{n+1})\ \ (\mathrm{mod}2\pi)\ , \tag{2b}$$

where the parameters α and β are $\alpha=mL^2\omega_0^2T$ and $\beta=T/mL^2$. The transition from weak (local) to strong (global) chaos occurs at $\alpha\beta\approx0.9716$ [13].

For the classical map [Eqs. (2a) and (2b)], small errors propagate as

$$\begin{bmatrix}\delta P_{n+1}\\ \delta\theta_{n+1}\end{bmatrix}=\mathbf{J}_n\begin{bmatrix}\delta P_n\\ \delta\theta_n\end{bmatrix}\ , \tag{3}$$

where

$$\mathbf{J}_n=\begin{bmatrix}1 & -\alpha\cos\theta_n\\ \beta & 1-\alpha\beta\cos\theta_n\end{bmatrix} \tag{4}$$

is the Jacobi linear stability matrix. Equation (3) implies that

$$\delta P_{n+1}^2=\delta P_n^2+(\alpha\cos\theta_n)^2\delta\theta_n^2-2(\alpha\cos\theta_n)\delta\theta_n\delta P_n\ , \tag{5a}$$

$$\delta\theta_{n+1}^2=(1-2\alpha\beta\cos\theta_n)\delta\theta_n^2+\beta^2\delta P_{n+1}^2+2\beta\delta\theta_n\delta P_n\ , \tag{5b}$$

wherein $\delta x^2\equiv(\delta x)^2$.

For maps in general, the largest Liapunov exponent is given by [14]

$$\lambda=\lim_{n\to\infty}\frac{1}{2n}\ln[\mathrm{Tr}(\mathbf{M}_n^{\dagger}\mathbf{M}_n)]\ , \tag{6}$$

where $\mathbf{M}_n=\mathbf{J}_{n-1}\mathbf{J}_{n-2}\cdots\mathbf{J}_0$ and $\mathbf{M}_n^{\dagger}$ is the adjoint of $\mathbf{M}_n$. A positive Liapunov exponent means that the magnitude of the error vector in phase space, defined as $d_n=\sqrt{\delta\theta_n^2+\delta P_n^2}$, grows exponentially with n [15]:

$$d_n=d_0\exp(\lambda n) \tag{7}$$

on the average provided that d_0 is sufficiently small and n is sufficiently large such that the linearized equation (3) is valid and convergence has been reached in Eq. (6).

III. WAVE-PACKET INITIAL MOTION AND SPREADING

Quantum mechanically, the time-dependent Schrödinger equation is also easily integrated to produce a mapping of the wave function from just before the nth kick to just before the $(n+1)$th kick [8]:

$$\Psi_{n+1}(\theta)=\hat{U}_K\hat{U}_V\Psi_n(\theta)\ , \tag{8}$$

where the operator

$$\hat{U}_V=\exp[i(\alpha/\hbar)\cos\theta] \tag{9}$$

describes the nth kick and the operator

$$\hat{U}_K=\exp[-i(\beta/2\hbar)P^2] \tag{10}$$

describes the free rotation in between kicks. The Floquet operator $\hat{F}=\hat{U}_K\hat{U}_V$ depends on two dimensionless parameters: $\alpha/\hbar$ and $\beta\hbar$. In the usual angular momentum representation, the Floquet matrix is 4π periodic in $\beta\hbar$. Thus we can, following the authors in [2], let $\beta\hbar\in(0,4\pi]$ without loss of generality.

The initial wave packet is chosen to be a series of identical, minimum-uncertainty Gaussians which are displaced along the θ axis by the integer multiples of 2π [8,10]:

$$\Psi_0(\theta)=\sum_{m=-\infty}^{\infty}(2\pi\sigma_0^2)^{-1/4}\exp\left[\frac{-(\theta-\theta_0-2\pi m)^2}{4\sigma_0^2}\right]\times\exp[ik_0(\theta-\theta_0-2\pi m)]\ , \tag{11}$$

where $\theta_0\in[0,2\pi]$. This series is a periodic function of θ with period 2π, satisfying the required periodic boundary condition. For $\sigma_0\ll1$, the initial wave packet is a very narrow Gaussian in the interval $[0,2\pi]$ with the following mean values and variances for the angular momentum and angle:

$$\langle P\rangle_0=\hbar k_0\ ,\ \ \Delta P_0^2=\hbar^2/4\sigma_0^2\ ,\ \ \langle\theta\rangle_0=\theta_0\ ,\ \ \Delta\theta_0^2=\sigma_0^2\ , \tag{12}$$

where, in general, $\Delta x\equiv(\langle x^2\rangle-\langle x\rangle^2)^{1/2}$ and $\Delta x^2\equiv(\Delta x)^2$.

Starting with the initial series of Gaussians (11), the quantum map (8) is iterated in the following way:

$$\Psi_{n+1}(\theta)=F_\theta\{\hat{U}_KF_P\{\hat{U}_V\Psi_n(\theta)\}\}\ , \tag{13}$$

where F_P denotes the Fourier transform of the quantity in the inner curly bracket from coordinate space to momentum space and F_θ denotes the inverse Fourier transform of the quantity in the outer curly bracket. If the cosine function in the kick operator $\hat{U}_V$ [Eq. (9)] is replaced by the first three terms of its Taylor series expansion about the center of the Gaussian which it acts on, i.e.,

$$\cos\theta \approx \cos(\theta_0+2\pi m)-(\theta-\theta_0-2\pi m)\sin(\theta_0+2\pi m) - \frac{(\theta-\theta_0-2\pi m)^2}{2}\cos(\theta_0+2\pi m) \quad (14)$$

and P^2 in the free operator, $\hat{U}_K$ [Eq. (10)], is rewritten as

$$P^2=\hbar^2k_1^2+2\hbar k_1(P-\hbar k_1)+(P-\hbar k_1)^2 , \quad (15)$$

then the quantum map (8) yields, after the first iteration,

$$\Psi_1(\theta)=\sum_{m=-\infty}^{\infty}(2\pi\Delta\theta_1^2)^{-1/4} \times\exp\left[\left[iA_1-\frac{1}{4\Delta\theta_1^2}\right](\theta-\theta_1-2\pi m)^2\right] \times\exp[ik_1(\theta-\theta_1-2\pi m)]\exp(i\Omega_1) , \quad (16)$$

where

$$A_1=\frac{1}{2\hbar\Delta\theta_1}\left[\Delta P_1^2-\frac{\hbar^2}{4\Delta\theta_1^2}\right]^{1/2}$$

and Ω_1 is a phase which is independent of θ. Like the initial wave packet, the wave packet after one iteration is also a series of shifted, identical Gaussians with k_1 and θ_1 given by one iteration of the classical map [see Eqs. (2a) and (2b)],

$$\hbar k_1=\hbar k_0-\alpha\sin\theta_0 , \quad (17a)$$

$$\theta_1=(\theta_0+\beta\hbar k_1) \pmod{2\pi} , \quad (17b)$$

and new variances given by

$$\Delta P_1^2=\Delta P_0^2+(\alpha\cos\theta_0)^2\Delta\theta_0^2 , \quad (18a)$$

$$\Delta\theta_1^2=(1-2\alpha\beta\cos\theta_0)\Delta\theta_0^2+\beta^2\Delta P_1^2 . \quad (18b)$$

Further iterations of the quantum map (8) according to Eq. (13) with the same approximation as in Eq. (14) preserve the form of the wave packet given by Eq. (16). The phase Ω_n gets more complicated but remains independent of θ, k_n and θ_n continue to evolve according to the classical map [(2a) and (2b)], and the variances evolve according to

$$\Delta P_{n+1}^2=\Delta P_n^2+(\alpha\cos\theta_n)^2\Delta\theta_n^2 -2(\alpha\cos\theta_n)\Delta\theta_n\Delta P_n\left[1-\frac{\hbar^2}{4\Delta\theta_n^2\Delta P_n^2}\right]^{1/2} , \quad (19a)$$

$$\Delta\theta_{n+1}^2=(1-2\alpha\beta\cos\theta_n)\Delta\theta_n^2 +\beta^2\Delta P_{n+1}^2+2\beta\Delta\theta_n\Delta P_n\left[1-\frac{\hbar^2}{4\Delta\theta_n^2\Delta P_n^2}\right]^{1/2} . \quad (19b)$$

If $\Delta\theta_n$ remains $\ll 1$, then the wave packet remains a narrow, but not minimum-uncertainty, Gaussian in the interval $[0,2\pi]$ with mean values and variances which evolve according to the classical map (2a) and (2b) and the variance map (19a) and (19b), respectively. Due to Heisenberg's uncertainty principle, the term under the square root in the variance map (19a) and (19b) is either zero or positive. Note that, except for the square-root terms, the variance map is identical in form to the classical-error map (5a) and (5b).

A careful analysis of the variance map (19a) and (19b) reveals that, under certain conditions, the time dependence of the variances is approximately that for a free rotor Gaussian wave packet, in agreement with our previous analytic study [8] which was verified numerically in [10]. Specifically, the angular momentum variance does not change from its initial value $\hbar^2/4\sigma_0^2$ and the angular variance grows quadratically with n,

$$\Delta\theta_n^2=\sigma_0^2+\frac{n^2\beta^2\hbar^2}{4\sigma_0^2} , \quad (20)$$

for one iteration provided that $\alpha\beta\ll\frac{1}{2}$ and $\sigma_0^2\ll\hbar/2\alpha$, and for $N>1$ iterations provided that $\alpha\beta\ll 1/2(N-1)$, $\sigma_0^2\ll\hbar/2\alpha$, and each of the $(N-1)$ preceding angular variances given by Eq. (20) is also $\ll\hbar/2\alpha$. The condition imposed on the product of the classical map parameters $\alpha\beta$ corresponds to weak chaos in the classical map.

These wave-packet results are, however, approximates because of the quadratic approximation made to the potential at each iteration [see Eq. (14)]. In our previous numerical study [10], initially well-localized (in position and momentum) wave packets given by Eq. (11) were propagated accurately utilizing the full Hamiltonian for the Floquet operator in an angular momentum representation. The expectation values of the exact packet were shown [10] to be well described by the classical map (2a) and (2b). The variances of the exact packet are also well approximated (see Table I for an example) by the iterates of the variance map (19a) and (19b). The functional form of the exact probability density (not presented here) is also well approximated by the series of Gaussians given by Eq. (16) wherein the subscript 1 is replaced by n. These approximations are no longer valid once the angular deviation has reached a saturation value of order 1 rad. From the variance map (19a) and (19b), we can easily deduce that

$$[\Delta\theta_{n+1}]_{\max}=(1+\alpha\beta)\Delta\theta_n+\beta\Delta P_n . \quad (21)$$

Equation (21) implies that the wave packet must be localized in both angle

$$\Delta\theta_n\ll\frac{1}{1+\alpha\beta} \quad (22a)$$

and angular momentum

$$\Delta P_n\ll\frac{1}{\beta} \quad (22b)$$

for $n=0,1,2,\ldots$ in order that the $(n+1)$th angular deviation is much less than order unity. Note that the term $(1+\alpha\beta)^{-1}$ in Eq. (22a) is always less than 1 since $\alpha\beta>0$. It follows from Eqs. (22a) and (22b) that the angular deviation must satisfy

$$\frac{\beta\hbar}{2}\ll\sigma_0\ll\frac{1}{1+\alpha\beta} \quad (23)$$

TABLE I. A comparison of the exact deviations for case (D) in Ref. [10] and the corresponding approximates obtained from the variance map (19a) and (19b). The following values were used: for Planck's constant, $\hbar=10^{-6}$; for the classical map parameters, $\alpha=0.005$, $\beta=50$; and for the wave-packet initial conditions, $\theta_0=\pi$, $k_0=251\,320$, and $\sigma_0=10^{-2}$. Note that the agreement between the exact and the approximate deviations diminishes as the angular deviation gets larger.

	Angular deviation (units of 10^{-2})		Angular momentum deviation (units of 10^{-5})	
Iteration	Exact	Approximate	Exact	Approximate
0	1.0000	1.0000	5.0000	5.0000
1	1.2747	1.2748	7.0709	7.0711
2	1.8977	1.8978	12.869	12.870
3	3.0048	3.0050	22.240	22.242
4	4.8652	4.8659	37.232	37.242
5	7.9411	7.9440	61.523	61.566
6	12.996	13.008	101.10	101.28
7	21.273	21.324	165.54	166.32

initially. However, the two inequalities in Eq. (23) cannot be simultaneously satisfied if $\beta\hbar/2 \geq (1+\alpha\beta)^{-1}$.

IV. AVERAGE KINETIC ENERGY OF A WELL-LOCALIZED WAVE PACKET

Next we consider the average kinetic energy of our well-localized wave packet in the very strongly chaotic regime ($\alpha\beta \gg 1$) of the classical map (2a) and (2b). The average kinetic energy is given by

$$\langle E \rangle_n = \frac{\langle P^2 \rangle_n}{2mL^2} = \frac{\langle P \rangle_n^2 + \Delta P_n^2}{2mL^2} . \tag{24}$$

Recall that the mean momentum $\langle P \rangle_n$ of the packet evolves according to the classical map ($\langle P \rangle_n \approx P_n$) and the time dependences of the angular momentum deviation ΔP_n are different in the presence of chaos and without chaos. The classical map can be treated as completely chaotic for $\alpha\beta \geq 5$ [6]. For this parameter range, the angular momentum deviation of our well-localized wave packet grows exponentially initially [10], while the angular momentum P_n of a single classical trajectory undergoes a random motion which is diffusive in character [6]. Thus the kinetic energy (24) is composed of an exponentially growing term plus a positive fluctuating part. Therefore, the kinetic energy of our well-localized wave packet does not grow diffusively (linearly) initially.

Equation (24) has two extreme limits. If the angular momentum deviation is small compared to the mean initially ($1/\sigma_0 \ll k_0$) and if it remains so, then $\langle E \rangle_n \approx \langle P \rangle_n^2 / 2mL^2$. Conversely, if the angular momentum deviation is large compared to the mean initially and if it remains so, then $\langle E \rangle_n \approx \Delta P_n^2 / 2mL^2$. A numerical example of the second case for $\alpha\beta=10$ is shown in Fig. 1, where the wave packet is initially centered at zero angle and zero angular momentum. As evident in Fig. 1, both the angular and the angular momentum deviations initially grow exponentially. The deviations were generated by the variance map (19a) and (19b) and they are in excellent agreement with exact numerical results, reported recently in [16], up to kick 13 before the exact angular deviation reaches its saturation value (~ 1.8) at kick 14. Also, during the first 13 kicks, the exact mean values are very close to zeros generated by the classical map.

The initially nondiffusive behavior of the kinetic energy of our wave packet is not in conflict with the diffusive behavior observed by other authors [2,11,12] previously. The apparent contradiction is due to (see also the discussion in [16]) the fact that our wave packet is different from those in [2,11,12]. Our wave packet is well localized in both angle and angular momentum, i.e., the deviations satisfy the inequalities in Eqs. (22a) and (22b), whereas the initial wave packets in [2,11,12] are not well localized. For instance, the ground state of the free rotor, which is typical of the initial states considered in [2,11,12], is uniformly distributed in angle. We emphasize that our present analytical analysis only indicates that the kinetic energy does not grow diffusively as long as the wave packet remains well localized. The question of whether diffusive growth sets in after this initial nondiffusive regime cannot be answered by our present analysis; one must resort to numerical means.

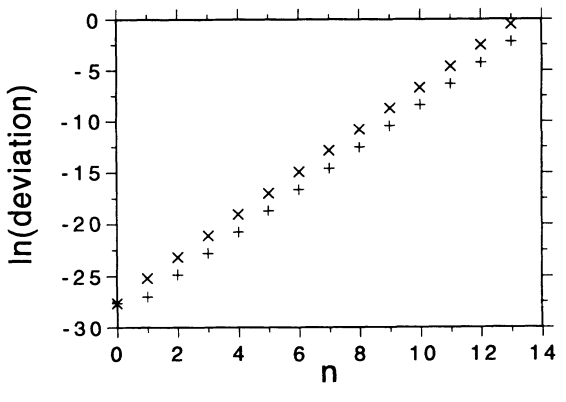

FIG. 1. A plot of the natural logarithm of the angular (×) and angular momentum (+) deviations versus n generated by the variance map (19a) and (19b). The following parameters were used: $\alpha=5/\pi$, $\beta=2\pi$, $\theta_0=k_0=0$, $\hbar=2\times10^{-24}$, and $\sigma_0=10^{-12}$.

V. INITIAL EXPONENTIAL GROWTH OF DEVIATIONS

In the presence of chaos, the product of the variances is much greater than its initial minimum value of $\hbar^2/4$ after the first few N iterations (typically one or two) because from numerical studies [10,16], we know that the deviations grow rapidly initially, on the average, exponentially with n until the angular deviation reaches a value of order unity:

$$\Delta\theta_n=\Delta\theta_0\exp(\chi n) \quad \text{and} \quad \Delta P_n=\Delta P_0\exp(\chi n) , \tag{25}$$

where χ is given by the average slope of the curve of the natural logarithm of the deviation versus n. Therefore, the square-root term in the variance map (19a) and (19b) is, to a very good approximation, equal to 1 after the first few N iterations. This means that the variance map has the same form as the classical-error map (5a) and (5b), or, in terms of the deviations,

$$\begin{bmatrix}\Delta P_{n+1}\\ \Delta\theta_{n+1}\end{bmatrix}\approx\mathbf{J}_n\begin{bmatrix}\Delta P_n\\ \Delta\theta_n\end{bmatrix} \quad \text{for } n=N,N+1,\ldots , \tag{26}$$

where $\mathbf{J}_n$ is the classical Jacobi matrix (4). Because the Jacobi matrix yields a positive Liapunov exponent λ [see Eq. (6)], like the magnitude of the classical errors (7), the magnitude of the quantum deviations, defined similarly as $D_n=\sqrt{\Delta\theta_n^2+\Delta P_n^2}$, also grows exponentially with n,

$$D_n=D_0\exp(\lambda n) , \tag{27}$$

on the average, provided that D_0 is sufficiently small and n is sufficiently large such that the variance map (19a) and (19b) is valid and convergence has been reached in Eq. (6). In order for Eq. (25) to be consistent with Eq. (27), we must evidently have $\chi=\lambda$. For the very strongly chaotic ($\alpha\beta\gg1$) regime of the classical map, Chirikov [1] has obtained an analytical estimate of the Liapunov exponent as a function of the classical map parameters:

$$\lambda=\ln\frac{\alpha\beta}{2} , \tag{28}$$

which is in close agreement with the exponent he determined numerically for $\alpha\beta\gtrsim6$. For $\alpha\beta=10$, $\lambda=1.609$ is quite close to the slopes, ~2.0, of the curves (straight lines) in Fig. 1. A better agreement is obtained [16] by using a transient Liapunov exponent λ_n rather than the asymptotic value $\lambda=\lambda_\infty$ of 1.609. Since the transient Liapunov exponent is defined and discussed thoroughly in [16], we will not repeat it here.

VI. EHRENFEST TIME

Using Eq. (25) and assuming the wave packet well-localized conditions in Eqs. (22a) and (22b), the Ehrenfest time (measured in kicks) in the presence of classical chaos can be easily estimated to be

$$N_E=\min\{N_\theta ,N_P\} , \tag{29}$$

where

$$N_\theta=\frac{1}{\lambda}\ln\frac{1}{(1+\alpha\beta)\sigma_0} \tag{30}$$

is the time it takes for the angular deviation to grow to $(1+\alpha\beta)^{-1}$ and

$$N_P=\frac{1}{\lambda}\ln\frac{1}{\beta\Delta P_0}=\frac{1}{\lambda}\ln\frac{2\sigma_0}{\beta\hbar} \tag{31}$$

is the time it takes for the momentum deviation to grow to β^{-1}. Three possibilities are implied by Eqs. (29)–(31):

$$N_E=N_P \Longleftrightarrow \sigma_0<\left|\frac{\beta\hbar}{2(1+\alpha\beta)}\right|^{1/2} , \tag{32a}$$

$$N_E=N_\theta=N_P \Longleftrightarrow \sigma_0=\left|\frac{\beta\hbar}{2(1+\alpha\beta)}\right|^{1/2} , \tag{32b}$$

$$N_E=N_\theta \Longleftrightarrow \sigma_0>\left|\frac{\beta\hbar}{2(1+\alpha\beta)}\right|^{1/2} . \tag{32c}$$

Due to Eq. (23), the square-root term in each of the three preceding equations satisfies

$$\frac{\beta\hbar}{2}\ll\left|\frac{\beta\hbar}{2(1+\alpha\beta)}\right|^{1/2}\ll\frac{1}{1+\alpha\beta} . \tag{33}$$

Of the three cases, case 2 [Eq. (32b)] gives the largest Ehrenfest time:

$$N_E=\frac{1}{2\lambda}\ln\frac{2}{\beta\hbar(1+\alpha\beta)} , \tag{34}$$

because in case 1 [Eq. (32a)], since σ_0 is bounded from above by the square-root term, N_E is bounded from above by Eq. (34), and in case 3 [Eq. (32c)], N_E is also bounded from above by Eq. (34), since σ_0 is bounded from below by the square-root term. The parameters used in Fig. 1 correspond to case 3 which predicts $N_E=15$, very close to 13 kicks which are observed.

Based on a semiclassical treatment of the kicked pendulum wave-packet dynamics, Chirikov, Israilev, and Shepelyansky [11] had also concluded that the rate of exponential spreading of an initially well-localized wave packet is determined by the Liapunov exponent, and also estimated that the Ehrenfest time is given by Eq. (29) (see also [6]). Their expression for N_P is identical to Eq. (31); however, their N_θ does not have the $1+\alpha\beta$ term that we have in Eq. (30). The discrepancy in the latter is due to different treatments of the wave packet spreading: classically by Chirikov, Israilev, and Shepelyansky, but quantum mechanically in this study.

VII. CONCLUDING REMARKS

We mention an exception to our general results presented here. Without the quadratic approximation to the potential in the Floquet operator in Eq. (8), it can be shown that $\hat{F}^2=\hat{I}$ (identity operator) when $\beta\hbar=2\pi$, and thus any wave function is periodic in time with a period of two kicks, independent of the value of the other Floquet parameter $\alpha/\hbar$. This means that, for instance, the mean values are likewise periodic independent of their in-

itial values, a behavior which is not exhibited by the classical map (2a) and (2b). This example is a special case of the quantum resonance (i.e., $\beta\hbar$ is a rational multiple of 4π) studied in [2,17]. Finally, Berman, Rubaev, and Zaslavsky [18] had previously stated that exponential spreading in angle of an initially well-localized wave packet at a rate given by the Liapunov exponent is to be expected for a kicked quantum oscillator in general when the classical limit yields chaotic motion. The analytical approach we have adopted here for the kicked pendulum can be applied to other kicked oscillators as well, and similar results are expected.

ACKNOWLEDGMENTS

I thank Professor R. F. Fox and Dr. T. C. Elston for helpful and illuminating discussions, and for providing their exact numerical results corresponding to the approximate ones in Fig. 1 for comparison.

[1] B. V. Chirikov, Phys. Rep. **52**, 263 (1979).

[2] G. Casati *et al.*, in *Stochastic Behavior in Classical and Quantum Hamiltonian Systems,* edited by G. Casati and J. Ford, Lecture Notes in Physics Vol. 93 (Springer-Verlag, Berlin, 1979).

[3] G. M. Zaslavsky, Phys. Rep. **80**, 157 (1981).

[4] B. Eckhardt, Phys. Rep. **163**, 205 (1988).

[5] C. Casati and L. Molinari, Theor. Phys. Suppl. **98**, 287 (1989).

[6] F. M. Izrailev, Phys. Rep. **196**, 299 (1990).

[7] L. E. Reichl, *The Transition to Chaos in Conservative Classical Systems: Quantum Manifestations* (Springer-Verlag, New York, 1992), Sec. 9.6.

[8] R. F. Fox and B. L. Lan, Phys. Rev. A **41**, 2952 (1990).

[9] Similar results have been obtained previously for a wave packet in a smooth potential: E. J. Heller, J. Chem. Phys. **62**, 1544 (1975); G. A. Hagedorn, Commun. Math. Phys. **71**, 77 (1980); M. Andrews, J. Phys. A **14**, 1123 (1981); R. G. Littlejohn, Phys. Rep. **138**, 193 (1986); see also the review in Sec. 7.1 of B. Eckhardt [4]. Similar results have also been obtained recently for the kicked Harper model: J. C. Kimball, V. A. Singh, and M. D'Souza, Phys. Rev. A **45**, 7065 (1992). It is worth noting that a wave-packet propagation method which goes beyond the quadratic approximation has recently been developed: see E. J. Heller and S. Tomsovic, Phys. Today **46** (7), 38 (1993), for a review and references.

[10] B. L. Lan and R. F. Fox, Phys. Rev. A **43**, 646 (1991). The exact numerical results presented in this reference correspond to the classical weakly chaotic regime only. Exact results for the strongly chaotic regime have also been calculated but are unpublished.

[11] B. V. Chirikov, F. M. Israilev, and D. L. Shepelyansky, Sov. Sci. Rev. C **2**, 209 (1981).

[12] D. L. Shepelyansky, Physica D **8**, 208 (1983).

[13] J. M. Greene, J. Math. Phys. **20**, 1183 (1979).

[14] P. Berge, Y. Pomeau, and C. Vidal, *Order Within Chaos: Towards a Deterministic Approach to Turbulence* (Wiley, New York, 1984), Appendix B.

[15] A. J. Lichtenberg and M. A. Lieberman, *Regular and Stochastic Motion* (Springer-Verlag, New York, 1983), Sec. 5.3.

[16] R. F. Fox and T. C. Elston, Phys. Rev. E **49**, 3683 (1994).

[17] F. M. Israilev and D. L. Shepelyansky, Theor. Math. Phys. **43**, 553 (1980).

[18] G. P. Berman, Y. V. Rubaev, and G. M. Zaslavsky, Nonlinearity **4**, 543 (1991); see also the discussion in Sec. 10.2 of G. M. Zaslavsky [3].